
JOURNAL OF THE AMERICAN CHEMICAL SOCIETY

Cyclic Peptides as Molecular Adapters for a Pore-Forming Protein

Jorge Sanchez-Quesada,^{†,‡} M. Reza Ghadiri,^{†,‡} Hagan Bayley,^{§,||} and Orit Braha^{*,§}

Contribution from the Departments of Chemistry and Molecular Biology, The Scripps Research Institute, La Jolla, California 92037, The Skaggs Institute for Chemical Biology, The Scripps Research Institute, La Jolla, California 92037, Department of Medical Biochemistry & Genetics, The Texas A&M University System Health Science Center, College Station, Texas 77843-1114, Department of Chemistry, Texas A&M University, College Station, TX 77843-3255

Received July 5, 2000

Abstract: Recently, cyclodextrins were shown to act as adapters for the pore-forming protein staphylococcal α -hemolysin (α HL). The bagel-shaped molecules bind in the lumen of the transmembrane channel formed by α HL and alter the properties of the pore. For example, the unitary conductance is reduced, and organic molecules can act as channel blockers by binding to the cavity within the cyclodextrin adapter. In a search for a class of adapters more versatile than the cyclodextrins and amenable to preparation as libraries, cyclic peptides have now been examined. Four peptides, *cyclo*[(L-Arg-D-Leu)₄-] ((RL)₄), *cyclo*[(L-Glu-D-Leu)₄-] ((EL)₄), *cyclo*[-(L-Phe-D-N-(aminoethyl)-Ala-L-Phe-D-Ala)₂-] (diNH₃⁺-(FA)₄), and *cyclo*[-(L-Phe-D-N-(carboxymethyl)-Ala-L-Phe-D-Ala)₂-] (diCO₂⁻-(FA)₄), became lodged within the α HL pore, altering the unitary conductance and ion selectivity. Further, the positively charged peptides, (RL)₄ and diNH₃⁺-(FA)₄, were able to act as binding sites for various small polyanions. For example, the second messenger IP₃ bound to (RL)₄ within the α HL pore. Therefore, the modulation of single-channel currents through pores containing cyclic peptide adapters may prove useful for sensing a variety of molecules.

Introduction

The ability to produce transmembrane channels and pores with tailored properties is a goal that is being pursued enthusiastically by both protein engineers and bioorganic chemists.¹ They seek the potential to mimic and extend the characteristics of natural channels and pores, such as permeation properties (the rates at which solutes of different size, shape, and charge move through a channel), gating (the means by

which channels open and close), and interactions with blockers (molecules that reduce or halt permeation, often by binding within the channel lumen). Engineered channels and pores are expected to have applications in biotechnology, especially as components of biosensors.²⁻⁸

Examples of the protein-engineering approach include work

(2) Braha, O.; Walker, B.; Cheley, S.; Kasianowicz, J. J.; Song, L.; Gouaux, J. E.; Bayley, H. *Chem. Biol.* **1997**, *4*, 497-505.

(3) Cornell, B. A.; Braach-Maksyutis, V. L. B.; King, L. G.; Osman, P. D. J.; Raguse, B.; Wiczorek, L.; Pace, R. J. *Nature* **1997**, *387*, 580-583.

(4) Motesharei, K.; Ghadiri, M. R. *J. Am. Chem. Soc.* **1997**, *119*, 11306-11312.

(5) Ziegler, C.; Göpel, W. *Curr. Opin. Chem. Biol.* **1998**, *2*, 585-591.
(6) Stora, T.; Lakey, J. H.; Vogel, H. *Angew. Chem., Int. Ed.* **1999**, *38*, 389-392.

(7) Gu, L.-Q.; Braha, O.; Conlan, S.; Cheley, S.; Bayley, H. *Nature* **1999**, *398*, 686-690.

(8) Bayley, H.; Braha, O.; Gu, L.-Q. *Adv. Mater.* **2000**, *12*, 139-142.

* Corresponding author. Email: obraha@medicine.tamu.edu.

[†] Departments of Chemistry and Molecular Biology, The Scripps Research Institute.

[‡] The Skaggs Institute for Chemical Biology, The Scripps Research Institute.

[§] Department of Medical Biochemistry & Genetics, The Texas A&M University System Health Science Center.

^{||} Department of Chemistry, Texas A&M University.

(1) Bayley, H. *Curr. Opin. Biotechnol.* **1999**, *10*, 94-103.

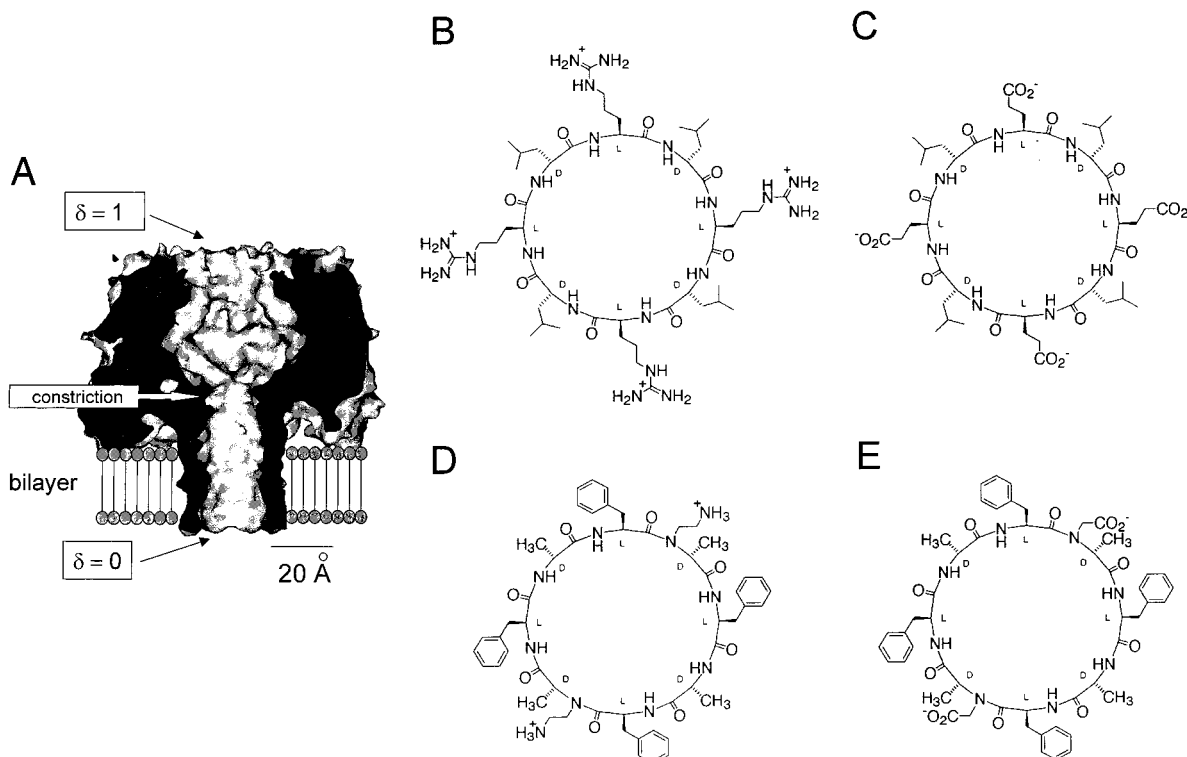


Figure 1. Structure of the α -hemolysin pore and the adapters used in this work. (a) Sagittal section through the heptameric pore in a lipid bilayer⁹ based on the crystal structure.⁹ The *cis* entrance of the 100 Å-long pore is ~ 70 Å above the lipid bilayer and is an opening ~ 30 Å in diameter. The *trans* entrance is close to the bilayer surface and is ~ 20 Å in diameter. The narrowest constriction in the lumen is about halfway through the channel, where the diameter is 14 Å.⁹ δ refers to the electrical distance (see Experimental Section: Data Analysis). (b) Structure of the eight-membered cyclic peptide *cyclo*-[(L-Arg-D-Leu)₄], (RL)₄. (c) *cyclo*-[(L-Glu-D-Leu)₄], (EL)₄. (d) *cyclo*-[(L-Phe-D-N-(aminoethyl)-Ala-L-Phe-D-Ala)₂], diNH₃⁺-(FA)₄. (e) *cyclo*-[(L-Phe-D-N-(carboxymethyl)-Ala-L-Phe-D-Ala)₂], diCO₂⁻-(FA)₄.

on staphylococcal α -hemolysin (α HL, α -toxin, Figure 1a), a 293-residue exotoxin that forms a mushroom-shaped heptameric pore in lipid bilayers.⁹ The α HL pore has a large conductance value (e.g., 500 pS in 0.5 M KCl, pH 7.0)¹⁰ and shows a weak preference for the transport of anions over cations.¹⁰ The pore allows the entry of molecules of ~ 3000 Da^{11–13} and their passage across the bilayer.^{14–16} Other studies have demonstrated that single-stranded, but not double-stranded, RNA and DNA molecules of far greater mass can be driven through the pore by an applied potential.^{17–20}

Earlier protein-engineering studies were largely focused on achieving control over assembly, which was done with altered α HL polypeptides that responded to proteases,²¹ metal ions,^{22,23}

light,²⁴ and chemical modification by site-specific alkylation.²⁵ More recent work has explored the fully assembled pore with particular attention to the placement of blocker sites in the channel lumen⁸ that respond to divalent metal ions^{2,22} and organic molecules.⁷ The finding that cyclodextrin adapters can be lodged within the channel lumen, where they continue to take part in host–guest interactions, is especially relevant to the present study.⁷ Cyclodextrins in the lumen also modify the ion selectivity of the α HL pore.²⁶

Examples of the bioorganic approach include peptide nanotubes made from cyclic peptides that stack in a predictable manner within the lipid bilayer to form well-defined channels.²⁷ The early examples contained an even number of alternating D- and L- α -amino acids.²⁸ Recently, new structures based on α -unsubstituted- β -chiral- β -amino acids have been introduced.²⁹ The transport properties of peptide nanotubes can be manipulated by altering the ring size. While the stacked 8-(α -amino acid)-membered rings transport small ions efficiently, the 10-membered *cyclo*[(L-Trp-D-Leu)₄-L-Gln-D-Leu] also transports

(9) Song, L.; Hobaugh, M. R.; Shustak, C.; Cheley, S.; Bayley, H.; Gouaux, J. E. *Science* **1996**, *274*, 1859–1865.

(10) Menestrina, G. *J. Membr. Biol.* **1986**, *90*, 177–190.

(11) Krasilnikov, O. V.; Sabirov, R. Z.; Ternovsky, V. I.; Merzliak, P. G.; Muratkhodjaev, J. N. *FEMS Microbiol. Immunol.* **1992**, *105*, 93–100.

(12) Bezrukov, S. M.; Vodyanov, I.; Brutyan, R. A.; Kasianowicz, J. J. *Macromolecules* **1996**, *29*, 8517–8522.

(13) Bezrukov, S. M.; Kasianowicz, J. J. *Eur. Biophys. J.* **1997**, *26*, 471–476.

(14) Füssle, R.; Bhakdi, S.; Szioegleit, A.; Tranum-Jensen, J.; Kranz, T.; Wellensiek, H.-J. *J. Cell Biol.* **1981**, *91*, 83–94.

(15) Bhakdi, S.; Muhly, M.; Füssle, R. *Infect. Immun.* **1984**, *46*, 318–323.

(16) Palmer, M.; Weller, U.; Messner, M.; Bhakdi, S. *J. Biol. Chem.* **1993**, *268*, 11963–11967.

(17) Kasianowicz, J. J.; Brandin, E.; Branton, D.; Deamer, D. W. *Proc. Natl. Acad. Sci. U.S.A.* **1996**, *93*, 13770–13773.

(18) Akeson, M.; Branton, D.; Kasianowicz, J. J.; Brandin, E.; Deamer, D. W. *Biophys. J.* **1999**, *77*, 3227–3233.

(19) Meller, A.; Nivon, L.; Brandin, E.; Golovchenko, J.; Branton, D. *Proc. Natl. Acad. Sci. U.S.A.* **2000**, *97*, 1079–1084.

(20) Deamer, D. W.; Akeson, M. *Trends Biotechnol.* **2000**, *18*, 147–151.

(21) Walker, B. J.; Bayley, H. *Protein Eng.* **1994**, *7*, 91–97.

(22) Walker, B.; Kasianowicz, J.; Krishnasastri, M.; Bayley, H. *Protein Eng.* **1994**, *7*, 655–662.

(23) Walker, B.; Braha, O.; Cheley, S.; Bayley, H. *Chem. Biol.* **1995**, *2*, 99–105.

(24) Chang, C.-Y.; Niblack, B.; Walker, B.; Bayley, H. *Chem. Biol.* **1995**, *2*, 391–400.

(25) Walker, B.; Bayley, H. *Protein Eng.* **1995**, *8*, 491–495.

(26) Gu, L.-Q.; Dalla Serra, M.; Vincent, J. B.; Vigh, G.; Cheley, S.; Braha, O.; Bayley, H. *Proc. Natl. Acad. Sci. U.S.A.* **2000**, *97*, 3959–3964.

(27) Hartgerink, J. D.; Clark, T. D.; Ghadiri, M. R. *Chem. Eur. J.* **1998**, *4*, 1367–1372.

(28) Ghadiri, M. R.; Granja, J. R.; Buehler, L. K. *Nature* **1994**, *369*, 301–304.

(29) Clark, T. D.; Buehler, L. K.; Ghadiri, M. R. *J. Am. Chem. Soc.* **1998**, *120*, 651–656.

glucose.³⁰ Size selectivity was also demonstrated with 8-(α -amino acid) ring nanotubes inserted into monolayers supported on gold.⁴ Small electroactive anions and cations such as $[\text{Fe}(\text{CN})_6]^{3-}$ and $[\text{Ru}(\text{NH}_3)_6]^{3+}$ had access to the gold surface, while large ions, such as $[\text{Mo}(\text{CN})_8]^{4-}$ did not.

Here we combine elements of both the protein-engineering and the bioorganic approaches, by using cyclic peptides as molecular adapters for the α HL pore. Unmodified cyclodextrins are readily available, but although surprisingly promiscuous, they are nevertheless limited in their ability to bind guest molecules.³¹ A vast array of modified cyclodextrins has been described.³² However, many commercial substituted cyclodextrins are complex mixtures of regioisomers with different extents of substitution.^{33,34} Therefore, we have sought alternative adapters, and here we test cyclic peptides. Rather than use the lipophilic peptides that by themselves form transmembrane pores,²⁷ we have tested hydrophilic peptides originally devised to cap the pores.³⁵ We show that cyclic peptides indeed act as adapters, which are able to alter the conductance and ion selectivity of the α HL pore, and serve as sites for the binding of blockers within the channel lumen.

Experimental Section

Protein Preparation. Wild-type α -hemolysin (α HL) was purified from the supernatant of a *Staphylococcus aureus* culture and heptamerized as described earlier.^{2,36} The experiments described here were initiated with both monomeric and heptameric α HL. The two forms of α HL yield single-channel currents with indistinguishable characteristics.²

Cyclic Peptide Synthesis. Cyclic peptide *cyclo*[(L-Arg-D-Leu)₄-] and *cyclo*[(L-Glu-D-Leu)₄-] ((RL)₄ and (EL)₄, Figure 1b, c) were prepared by linear synthesis on a solid support by using acid-labile hydroxy-functionalized Wang resin and standard fluorenylmethoxycarbonyl (Fmoc) chemistry.³⁷ Linear peptides were cleaved from the resin in a mixture of trifluoroacetic acid/water (20:1) containing phenol, ethanedithiol, and thioanisole (0.75, 0.25, and 0.50 g, respectively, in 10 mL of the hydrolytic solution) at 0 °C for 2 h and then cyclized in DMF at a concentration of 1 mM with HATU and HOAt as activating agents at 0 °C.³⁸ Removal of the side-chain protecting groups (*p*-methylphenylsulfonate for arginine in (RL)₄ and benzyl for glutamate in (EL)₄) was performed in HF/anisole (10:1) at 0 °C for 2 h. Cyclic peptides were further purified by reverse phase HPLC (C4 column eluted with trifluoroacetic acid/acetonitrile/water) and characterized by MS ((RL)₄ positive ES-MS: $[\text{M} + \text{H}^+] = 1078$, negative ES-MS: $[\text{M} + \text{trifluoroacetate}^-] = 1190$; (EL)₄ positive ES-MS: $[\text{M} + \text{Na}^+] = 992$, negative ES-MS: $[\text{M} - \text{H}^+]^- = 968$).

The diammonium and dicarboxylate cyclic peptides, *cyclo*[(L-Phe-D-N-(aminoethyl)-Ala-L-Phe-D-Ala)₂-] and *cyclo*[(L-Phe-D-N-(carboxymethyl)-Ala-L-Phe-D-Ala)₂-], (diNH₃⁺-(FA)₄ and diCO₂⁻-(FA)₄, Figure 1d, e), were prepared on a solid support (Pam resin) by using BOC chemistry. BOC dipeptides, including the *N*-alkyl groups protected as phthalimide or methyl ester functions, were synthesized in solution and then used as building blocks for the preparation of the linear peptides.³⁵ After cleavage from the resin with HF/anisole (10:1) at 0

°C for 1 h, the peptides were cyclized in DMF, as above, and the protecting groups on the secondary amides were removed. The phthalimido groups on the *N*-ethylamino groups were cleaved with hydrazine monohydrate (500 equiv) in ethanol at room temperature for 4 h, while the methyl esters were hydrolyzed with LiOH in water/THF (1:6) at room temperature for 18 h to yield the *N*-carboxymethyl groups. The cyclic peptides were purified by reverse phase HPLC (C4 column eluted with trifluoroacetic acid/acetonitrile/water) and characterized by MS (diNH₃⁺-(FA)₄ positive ES-MS: $[\text{M} + \text{H}^+] = 960$, negative ES-MS: $[\text{M} + \text{Cl}^-] = 994$; diCO₂⁻-(FA)₄ positive ES-MS: $[\text{M} + \text{Na}^+] = 1011$, negative ES-MS: $[\text{M} - \text{H}^+]^- = 987$).

The cyclic peptides (RL)₄ and diNH₃⁺-(FA)₄ were dissolved in 0.5 M KCl, 5 mM Hepes, pH 7.5, to form 2 mM and 1 mM stock solutions, respectively. The cyclic peptides (EL)₄ and diCO₂⁻-(FA)₄ were dissolved in water at 1 mM, by titrating to neutral pH with 1 M KOH.

Additional Materials. Various small molecules were tested as channel blockers. Mellitic acid (1,2,3,4,5,6-benzenehexacarboxylic acid, hexacarboxybenzene; Aldrich, Milwaukee, WI), *L*-myo-inositol 1,4,5-tris-phosphate hexapotassium salt (*L*-IP₃; Sigma, St. Louis, MO) and *D*-myo-inositol 1,4,5-tris-phosphate hexasodium salt (*D*-IP₃; Alexis, San Diego, CA) were dissolved in water to form 10 mM stock solutions. Phytic acid (*myo*-inositol hexakis(dihydrogen phosphate), IP₆; Aldrich) was purchased as a 40% (w/v) solution in water and further diluted with water to 10 mM.

Bilayer Recordings. A bilayer of 1,2-diphytanoyl-*sn*-glycero-3-phosphocholine (Avanti Polar Lipids, Alabaster, AL) was formed by the method of Montal and Mueller³⁹ on a 100–150 μm orifice in a 25 μm -thick Teflon film (Goodfellow Corporation, Malvern, PA) separating the two chambers of a Teflon planar bilayer apparatus. Each chamber contained 2 mL of 0.5 M KCl (Mallinckrodt, St. Louis, MO), 5 mM MOPS (American Bioanalytical, Natick, MA) titrated to pH 7.5 with KOH. Monomeric WT- α HL (final concentration 50–100 ng mL⁻¹) or heptameric WT- α HL (final concentration 3–15 ng mL⁻¹) was added to the *cis* compartment. In both cases, heptameric pores assemble into the bilayer. The chamber was stirred until a single channel appeared, as described previously.² Transmembrane currents were recorded with a model 3900A integrated patch clamp amplifier (Dagan Corporation, Minneapolis, MN) with a built-in four-pole Bessel filter set at 10 kHz. For some experiments an Axopatch-1D amplifier (Axon Instruments, Foster City, CA) was used. The electrodes were Ag/AgCl in 1.5% agarose (BioRad, Hercules, CA) containing 3 M KCl. The *cis* chamber was at virtual ground. A positive potential indicates a higher potential in the *trans* chamber, and a positive current is one in which cations flow from the *trans* to the *cis* chamber. For analysis, the currents were further low-pass filtered with an eight-pole Bessel filter (model 902 Frequency Devices, Haverhill, MA) with the corner frequency set between 3 and 10 kHz (–3 dB), and sampled by computer at 10–333 kHz with a Digidata 1200 A/D converter (Axon Instruments). Cyclic peptides and various small molecule blockers were pipeted into the *cis* or *trans* chamber, as indicated, to give the final concentrations specified in the text. The addition of unbuffered blocker solutions (see above) reduced the pH in the chamber by no more than 0.1 units.

Data Analysis. Data were analyzed and presented by using the software pClamp6.0 or pClamp7.0 (Axon Instruments) and Origin5.0 (Microcal, Northampton, MA). Mean values with standard deviations are quoted. Conductance values were obtained from the peaks of all-point histograms or measured manually when the number of events was low. Mean residence times (τ values) were obtained from dwell-time histograms by fitting the distributions to exponential functions. Where necessary, very short events (30 to 80 μs) were identified and measured manually, to prevent the underestimation of dwell times by the software. The adjusted data sets were then exported to Origin5.0 for the construction of dwell-time histograms. Numerical data are given with standard deviations; *n* values refer to the number of independent experiments. Values for conductance are given to three significant figures, and kinetic constants, to two significant figures.

The electrical distance (δ) from the *trans* side of the bilayer was measured for peptides according to the approach of Woodhull^{40,41} from

(30) Granja, J. R.; Ghadiri, M. R. *J. Am. Chem. Soc.* **1994**, *116*, 10785–10786.

(31) Rekharsky, M. V.; Inoue, Y. *Chem. Rev.* **1998**, *98*, 1875–1917.

(32) Khan, A. R.; Forgo, R.; Stine, K. J.; D'Souza, V. T. *Chem. Rev.* **1998**, *98*, 1977–1996.

(33) Tanaka, Y.; Kishimoto, Y.; Terabe, S. *Anal. Sci.* **1998**, *14*, 383–388.

(34) Tanaka, Y.; Terabe, S. *J. Chromatogr.* **1997**, *781*, 151–160.

(35) Sanchez-Quesada, J.; Isler, M. P.; Ghadiri, M. R. Manuscript in preparation.

(36) Walker, B. J.; Krishnaswamy, M.; Zorn, L.; Kasianowicz, J. J.; Bayley, H. *J. Biol. Chem.* **1992**, *267*, 10902–10909.

(37) Fields, G. B.; Noble, R. L. *Int. J. Pept. Protein Res.* **1990**, *35*, 161–214.

(38) Clark, T. D.; Buriak, J. M.; Kobayashi, K.; Isler, M. P.; McRee, D. E.; Ghadiri, M. R. *J. Am. Chem. Soc.* **1998**, *120*, 8949–8962.

(39) Montal, M.; Mueller, P. *Proc. Natl. Acad. Sci. U.S.A.* **1972**, *69*, 3561–3566.

the slope of the line obtained by plotting:

$$\ln K_d(V) = \ln K_d(0) - z\delta FV/RT \quad (1)$$

where z is charge on the peptide, V is applied potential, and F , R , T have their usual meanings. The slopes were obtained from linear fits by the method of least squares (Origin5.0) to data obtained at low applied potentials, under which the cyclic peptides both associate and dissociate from the *trans* side of the bilayer (see Figures 2e, 3e, and 4d). If the potential is assumed to drop linearly from the *trans* ($\delta = 0$) to the *cis* ($\delta = 1$) entrance of the pore (Figure 1a), the actual distance from the *trans* side of the bilayer to the binding site of the peptide is δh , where h is the distance between the two entrances. Obviously this is an oversimplification (see Discussion and, for example, ref 42).

Charge Selectivity. Charge selectivities, expressed as permeability ratios P_{K^+}/P_{Cl^-} , were determined from measurements of reversal potentials in asymmetric solutions. Ionic concentrations were converted to ionic activities⁴³ and substituted into the Goldman–Hodgkin–Katz equation (GHK)⁴¹ to obtain P_{K^+}/P_{Cl^-} . Experiments were initiated under symmetrical conditions (e.g., with 0.5 M KCl in both chambers), and any electrode offset was balanced. Asymmetrical conditions were then obtained by adding concentrated KCl to the *cis* chamber to bring the final concentration to 0.9–1.3 M KCl. I – V data were then recorded. In each experiment, the reversal potentials for both the unoccupied α HL pore and the pore with a cyclic peptide lodged in it were determined.

Results

The α HL Pore and Cyclic Peptide Adapters. The wild-type α -hemolysin pore was used in this work. A sagittal section through the heptameric pore reveals a central 100 Å-long channel with a constriction about halfway through the lumen, where the diameter is reduced to 14 Å (Figure 1a). Four peptide adapters (Figure 1b–e), which were found to lodge in the lumen of the pore, were tested here. The peptides carry the following overall charge at neutral pH: (RL)₄, +4; (EL)₄, –4; diNH₃⁺-(FA)₄, +2; diCO₂[–]-(FA)₄, –2.

Cyclic Peptides Lodge in the α HL Channel Causing a Reduction in Unitary Conductance. Planar bilayers of 1,2-diphytanoyl-*sn*-glycero-3-phosphocholine were formed in an aperture in a Teflon partition separating two chambers containing 0.5 M KCl, 5 mM MOPS, pH 7.5. Under these conditions, at an applied potential of +80 mV, a single α HL channel shows a steady conductance of about 500 pS.¹⁰ In the presence of the cyclic peptide (RL)₄ (20 μ M, *trans*) transient reductions in current were observed ($\tau_{\text{off}} = 1.6 \pm 0.1$ ms, $n = 6$) during which the open channel conductance was reduced from 500 ± 14 pS ($n = 6$) to 231 ± 5 pS ($n = 6$) (Figure 2a, b). At a constant applied potential, the concentration dependence of the events (Figure 2a) was consistent with a simple bimolecular kinetic scheme (Scheme 1), for example at +80 mV $k_{\text{on}} = 1.1 (\pm 0.2) \times 10^6 \text{ M}^{-1} \text{ s}^{-1}$, $k_{\text{off}} = 620 (\pm 70) \text{ s}^{-1}$, $K_d = 540 (\pm 60) \mu\text{M}$ ($n = 6$).

The current reductions were frequent only at positive applied potentials, suggesting that the positively charged (RL)₄ is driven into the channel by the potential (Figure 2c). The extent of reduction in unitary conductance was $53 \pm 2\%$ ($n = 3$) between +10 and +100 mV, as measured from the ratio of the slopes of I – V curves (for example Figure 2d). At constant (RL)₄ concentrations, the frequency of occurrence of the current reduction events increased with increasing positive potential as

did the dwell time of the cyclic peptide (Table 1, Figure 2c), for example $k_{\text{on}} +40 \text{ mV} = 0.48 (\pm 0.14) \times 10^6 \text{ M}^{-1} \text{ s}^{-1}$ ($n = 5$), $k_{\text{on}} +100 \text{ mV} = 1.4 (\pm 0.1) \times 10^6 \text{ M}^{-1} \text{ s}^{-1}$ ($n = 6$); $k_{\text{off}} +40 \text{ mV} = 2500 (\pm 300) \text{ s}^{-1}$ ($n = 5$), $k_{\text{off}} +100 \text{ mV} = 380 (\pm 10) \text{ s}^{-1}$ ($n = 6$). Both kinetic parameters thus contribute to a significant increase in K_d with increased positive applied potential (Figure 2e): $K_d +40 \text{ mV} = 5.2 (\pm 1.1) \text{ mM}$ ($n = 5$), $K_d +100 \text{ mV} = 0.28 (\pm 0.02) \text{ mM}$ ($n = 6$). A calculation of the electrical distance (δ) for the site of peptide binding according to Woodhull^{40,41} gave $\delta = 0.39 \pm 0.04$ ($n = 5$), where $\delta = 0$ on the *trans* side of the bilayer (Figure 1a). At applied potentials above +100 mV, the peptide was driven through the pore with a consequent increase in K_d (Figure 2e), as described more fully below for the case of diCO₂[–]-(FA)₄.

The behavior of the diammonium cyclic peptide diNH₃⁺-(FA)₄ was consistent with that of (RL)₄ (Figure 3). When added to the *trans* side of the bilayer, diNH₃⁺-(FA)₄ also produced reductions in unitary conductance, which increased in duration when positive potentials were applied. The extent of reduction in unitary conductance was $66 \pm 7\%$ ($n = 4$). This value was obtained from the ratio of the slopes of the I – V curves, although they become nonlinear at high potentials (Figure 3). A linear relationship between the frequency of occurrence of the peptide-binding events ($P_{\alpha\text{HL-peptide}}/P_{\alpha\text{HL}}$) and the peptide concentration was again indicative of a bimolecular interaction (Figure 3c). Interestingly, at high peptide concentrations, a second class of events was observed (Figure 3a), which occurred at a frequency proportional to the square of the peptide concentration (Figure 3d), suggesting that a second molecule of diNH₃⁺-(FA)₄ can become lodged in the lumen of the α HL pore.

At a constant diNH₃⁺-(FA)₄ concentration, the frequency of occurrence of the primary events again increased with increasing positive potential as did the dwell time of the cyclic peptide (Table 2), for example $k_{\text{on}} +40 \text{ mV} = 0.92 (\pm 0.07) \times 10^6 \text{ M}^{-1} \text{ s}^{-1}$ ($n = 4$), $k_{\text{on}} +100 \text{ mV} = 1.3 (\pm 0.1) \times 10^6 \text{ M}^{-1} \text{ s}^{-1}$ ($n = 4$); $k_{\text{off}} +40 \text{ mV} = 360 (\pm 10) \text{ s}^{-1}$ ($n = 4$), $k_{\text{off}} +100 \text{ mV} = 74 (\pm 18) \text{ s}^{-1}$ ($n = 4$); $K_d +40 \text{ mV} = 0.420 (\pm 0.03) \text{ mM}$ ($n = 4$), $K_d +100 \text{ mV} = 0.043 (\pm 0.003) \text{ mM}$ ($n = 4$). A calculation of the electrical distance (δ) for the site of peptide binding gave $\delta = 0.38 \pm 0.01$ ($n = 4$).

Negatively charged cyclic peptides are also able to interact with the lumen of the α HL pore to produce reductions in unitary conductance. In the case of (EL)₄, the currents observed while the peptide was bound were less stable than in the case of (RL)₄. The addition of EDTA did not change the response to (EL)₄. Therefore, metal ion contaminants are unlikely to be the source of the more erratic currents. Application of (EL)₄ to the *trans* side of the membrane resulted in short blocking events that were detected only at negative potentials, again consistent with the peptide being driven into the α HL pore by the applied potential, for example at –100 mV, $88 \pm 5\%$ block, $k_{\text{on}} = 5.7 (\pm 1.7) \times 10^4 \text{ M}^{-1} \text{ s}^{-1}$, $k_{\text{off}} = 580 (\pm 130) \text{ s}^{-1}$, $K_d = 10 (\pm 3) \text{ mM}$ ($n = 5$).

In the case of diCO₂[–]-(FA)₄, in which the charged groups are located on the nitrogens of the peptide backbone, interaction with the α HL pore produced a reduction in unitary conductance of $90 \pm 2\%$ ($n = 4$) over the range –10 to –150 mV (Figure 4a, b). The frequency of occurrence of peptide-binding events depends linearly on the concentration of the peptide, indicative of a bimolecular interaction (Figure 4c). The voltage dependence of the interaction of diCO₂[–]-(FA)₄ with α HL exhibited interesting behavior at high potentials. As expected, k_{on} increased at negative potentials (Table 3). Surprisingly, k_{off} first decreased and then increased (Table 3). The combined effect on K_d was

(40) Woodhull, A. M. *J. Gen. Physiol.* **1973**, *61*, 687–708.

(41) Hille, B. *Ionic Channels of Excitable Membranes*; Sinauer: Sunderland, MA, 1991.

(42) Syganow, A.; von Kitzing, E. *Biophys. J.* **1999**, *76*, 768–781.

(43) Zemaitis, J. F.; Clark, D. M.; Rafal, M.; Scriver, N. *Handbook of Aqueous Electrolyte Thermodynamics: Theory and Application*; American Institute of Chemical Engineers: New York, 1986.

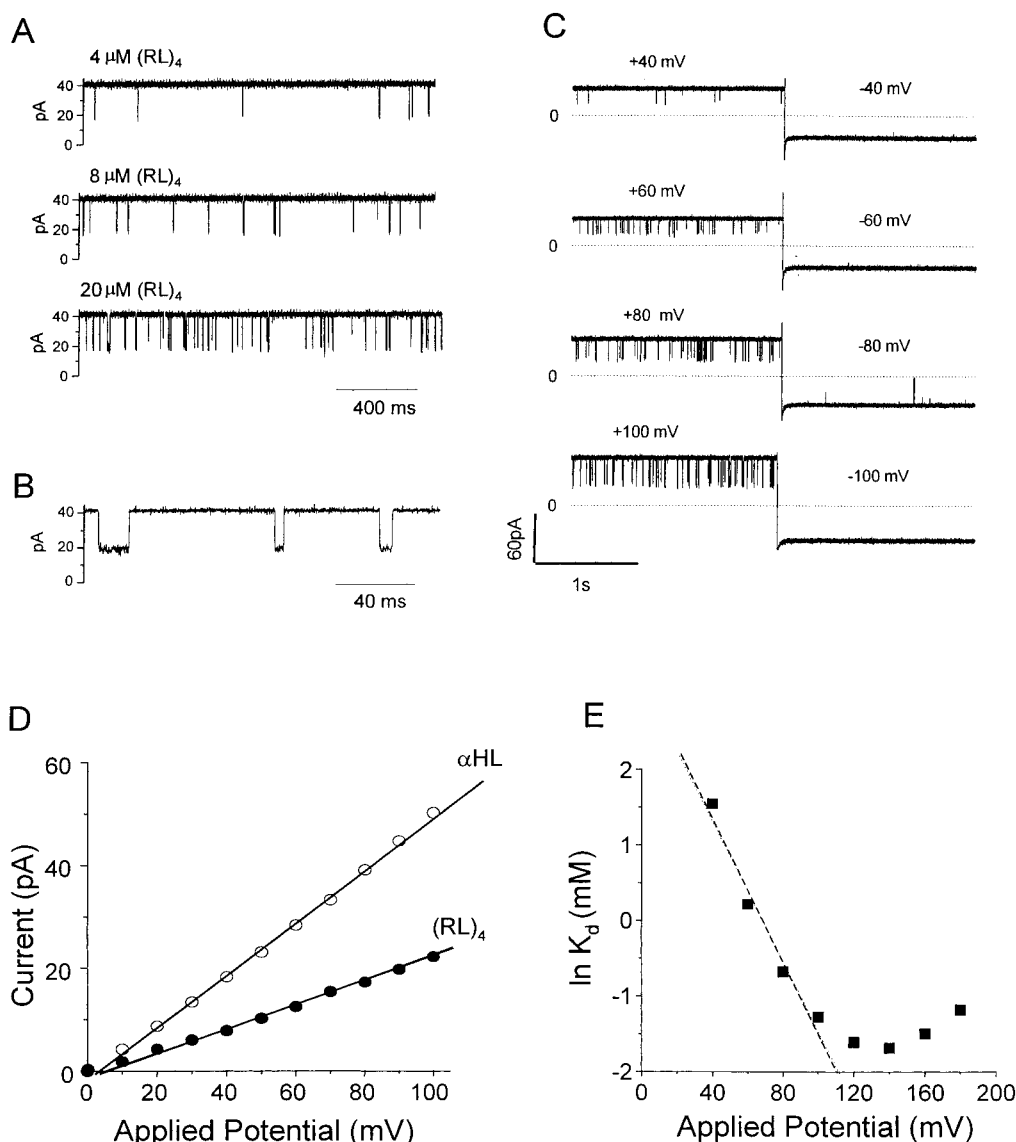
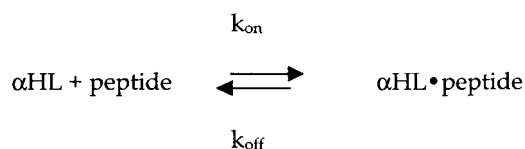


Figure 2. Interaction of the cyclic peptide $(RL)_4$ with the αHL pore. (a) Dose dependence of the blocking events at a constant voltage (+80 mV). The frequency of occurrence of the blocking events (downward deflections) increases with increasing $(RL)_4$ concentration. Signals were Bessel filtered at 2 kHz and acquired at 10 kHz. (b) Expanded trace of events in (a) ($20 \mu M (RL)_4$) reveals discrete steps of decreased conductance. (c) Voltage dependence of the occurrence of the blocking events at a constant $(RL)_4$ concentration ($20 \mu M$). The blocking events occur at positive potentials but rarely at negative potentials. (d) The residual current when $(RL)_4$ is lodged in the channel is proportional to the applied potential. Current–voltage (I – V) relationships for unoccupied αHL (\circ), and for αHL with $(RL)_4$ lodged in the channel lumen (\bullet), measured in the same experiment. (e) Voltage dependence of the dissociation constant of $(RL)_4$ ($K_d = k_{off}/k_{on}$). The data at low applied potentials are fitted to eq 1 (dashed line).

Scheme 1



an increase in affinity of $diCO_2^{--}(FA)_4$ at low negative potentials but a decrease in affinity at high potentials (Table 3, Figure 4d). Most probably, at high negative potentials, $diCO_2^{--}(FA)_4$ is forced through the central constriction in the channel lumen and exits through the *cis* entrance. A calculation of the electrical distance (δ) for the site of peptide binding, using K_d values obtained at low potentials, gave $\delta = 0.49 \pm 0.09$ ($n = 4$).

Cyclic Peptide Adapters Alter the Ion Selectivity of the αHL Pore. We tested the effects of placing peptide adapters in the channel lumen on charge selectivity. The αHL pore is weakly anion selective. Reversal potentials were determined

from single-channel I – V relationships obtained with asymmetric KCl concentrations and used to calculate ionic permeability ratios with the GHK equation. In the case of $(RL)_4$, we found $P_{K^+}/P_{Cl^-} = 0.75 \pm 0.11$ ($n = 3$) for the unoccupied pore, and in the same three experiments, $P_{K^+}/P_{Cl^-} = 0.43 \pm 0.06$ ($n = 3$) during $(RL)_4$ occupancy events (Figure 5a). Similarly, for $diNH_3^+(FA)_4$, we found $P_{K^+}/P_{Cl^-} = 0.48 \pm 0.01$ ($n = 3$) (Figure 5b). Hence, the positively charged adapters, $(RL)_4$ and $diNH_3^+(FA)_4$, contribute to an increase in the anion selectivity of the αHL pore. In keeping with a Coulombic effect, when $(EL)_4$ was lodged within the lumen, the αHL pore became cation selective $P_{K^+}/P_{Cl^-} = 1.76 \pm 0.33$ ($n = 3$) (Figure 5c).

The Cyclic Peptide Adapters Form Binding Sites for Channel Blockers within the Lumen of the αHL Pore. To test whether a cyclic peptide would act as a molecular adapter by forming a site to which channel blockers bind, we focused on the properties of the positively charged adapters $(RL)_4$ and

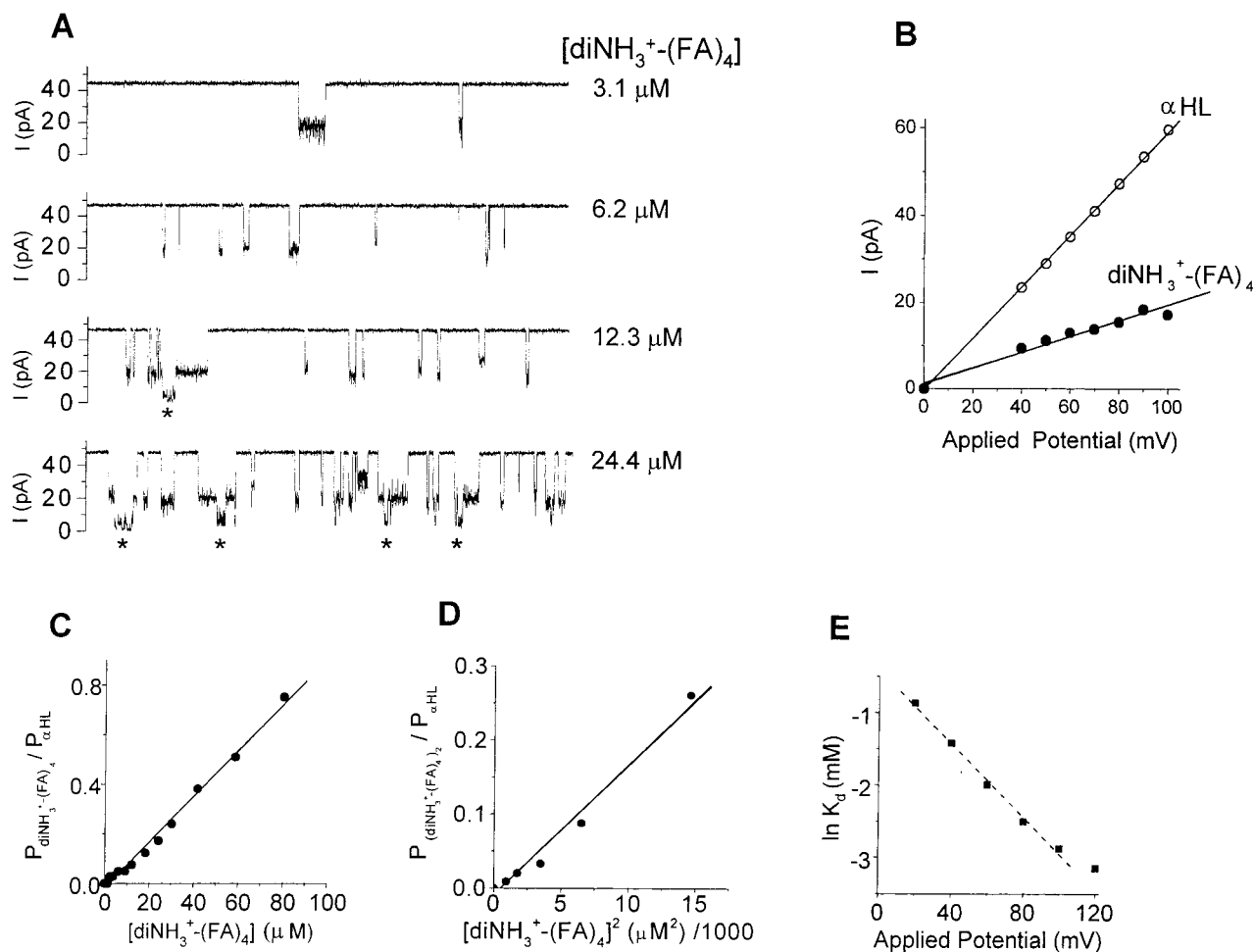


Figure 3. Interaction of the cyclic peptide $\text{diNH}_3^+(\text{FA})_4$ with the αHL pore. (a) Frequency of $\text{diNH}_3^+(\text{FA})_4$ -binding events depends on the concentration of the cyclic peptide in solution. The concentrations of $\text{diNH}_3^+(\text{FA})_4$ in the *trans* chamber were 3.1, 6.2, 12.3, and 24.4 μM . Events produced by the binding of two molecules of cyclic peptide within the αHL channel appear as almost complete blockades of the pore (*, at 12.3 μM and 24.4 μM peptide). The currents were recorded at +80 mV. Bessel filter, 2 kHz; acquisition rate, 5 kHz. (b) Residual current when $\text{diNH}_3^+(\text{FA})_4$ is lodged in the channel is proportional to the applied potential. I - V relationships for unoccupied αHL (\circ), and for αHL with $\text{diNH}_3^+(\text{FA})_4$ lodged in the channel lumen (\bullet), measured in the same experiment. (c) The binding of $\text{diNH}_3^+(\text{FA})_4$ to αHL is concentration dependent. Plot of $P_{\alpha\text{HL-peptide}}/P_{\alpha\text{HL}}$ versus the concentration of $\text{diNH}_3^+(\text{FA})_4$ in the *trans* chamber at an applied potential of +80 mV. (d) Plot of $P_{\alpha\text{HL-peptide}}/P_{\alpha\text{HL}}$ versus the square of the concentration of $\text{diNH}_3^+(\text{FA})_4$ under the same conditions as those of (c). (e) Voltage dependence of the first K_d for $\text{diNH}_3^+(\text{FA})_4$. The data at low applied potentials are fitted to eq 1 (dashed line).

Table 1. Kinetic Data for the Interaction of $(\text{RL})_4$ with the αHL Pore^a

V (mV)	k_{on} ($\text{M}^{-1}\text{s}^{-1}$)	k_{off} (s^{-1})	K_d (μM)
40	$0.48 (\pm 0.14) \times 10^6$	2500 ± 300	5200 ± 1100
60	$0.78 (\pm 0.13) \times 10^6$	1000 ± 200	1300 ± 400
80	$1.1 (\pm 0.2) \times 10^6$	620 ± 70	540 ± 60
100	$1.4 (\pm 0.1) \times 10^6$	380 ± 10	280 ± 20
120	$1.7 (\pm 0.2) \times 10^6$	240 ± 20	150 ± 30
140	$1.9 (\pm 0.2) \times 10^6$	350 ± 40	190 ± 40

^aData are averaged from four experiments and given to two significant figures.

$\text{diNH}_3^+(\text{FA})_4$, which produce less extensive, longer, and more uniform changes in unitary conductance than $(\text{EL})_4$ and $\text{diCO}_2^-(\text{FA})_4$. We speculated that bulky negatively charged molecules might interact with positively charged adapters lodged within the channel lumen.

Experiments with $(\text{RL})_4$ were carried out at +80 mV and +100 mV, where the longer dwell time of $(\text{RL})_4$ facilitates observation. Although the addition of blockers to the *trans* chamber produced signals, we favored addition to the *cis* chamber whence a positive potential pulls negatively charged analytes into the channel lumen. The addition of mellitic acid

(1,2,3,4,5,6-benzenehexacarboxylic acid) to the *cis* chamber in the presence of 6 μM *trans* $(\text{RL})_4$ resulted in rapid dose-dependent fluctuations that appeared only during the $(\text{RL})_4$ binding events resulting in a $90 \pm 2\%$ ($n = 7$) overall block of the current, compared with the 53% reduction by $(\text{RL})_4$ in the absence of blocker (Figure 6ab). At a constant potential of +80 mV, the frequency of occurrence of mellitic acid binding events increased linearly with concentration. The kinetic parameters for the association of mellitic acid with $\alpha\text{HL} \cdot (\text{RL})_4$ at +80 mV were: $k_{\text{on}} = 2.8 \pm 0.6 \times 10^7 \text{ M}^{-1} \text{ s}^{-1}$, $k_{\text{off}} = 5700 \pm 800 \text{ s}^{-1}$, $K_d = 210 \pm 50 \mu\text{M}$ ($n = 7$).

The binding of phytic acid (IP_6) was examined in the same way (Figure 6c): at +100 mV, $94 \pm 1\%$ block, $k_{\text{on}} = 2.3 \pm 0.3 \times 10^7 \text{ M}^{-1} \text{ s}^{-1}$, $k_{\text{off}} = 2900 \pm 700 \text{ s}^{-1}$, $K_d = 130 \pm 40 \mu\text{M}$ ($n = 8$). The L and D forms of IP_3 (Figure 6c) were not distinguishable from each other: L- IP_3 +100 mV, $82 \pm 6\%$ block, $k_{\text{on}} = 5.4 \pm 1.8 \times 10^6 \text{ M}^{-1} \text{ s}^{-1}$, $k_{\text{off}} = 1.3 \pm 0.4 \times 10^4 \text{ s}^{-1}$, $K_d = 2.4 \pm 0.3 \text{ mM}$ ($n = 4$); D- IP_3 +100 mV, $85 \pm 3\%$ block, $k_{\text{on}} = 3.6 \pm 1.6 \times 10^6 \text{ M}^{-1} \text{ s}^{-1}$, $k_{\text{off}} = 1.1 \pm 0.6 \times 10^4 \text{ s}^{-1}$, $K_d = 3.1 \pm 1.5 \text{ mM}$ ($n = 6$).

The interaction of IP_6 with $\text{diNH}_3^+(\text{FA})_4$, lodged in the lumen of the pore, was also examined by the addition of the blocker

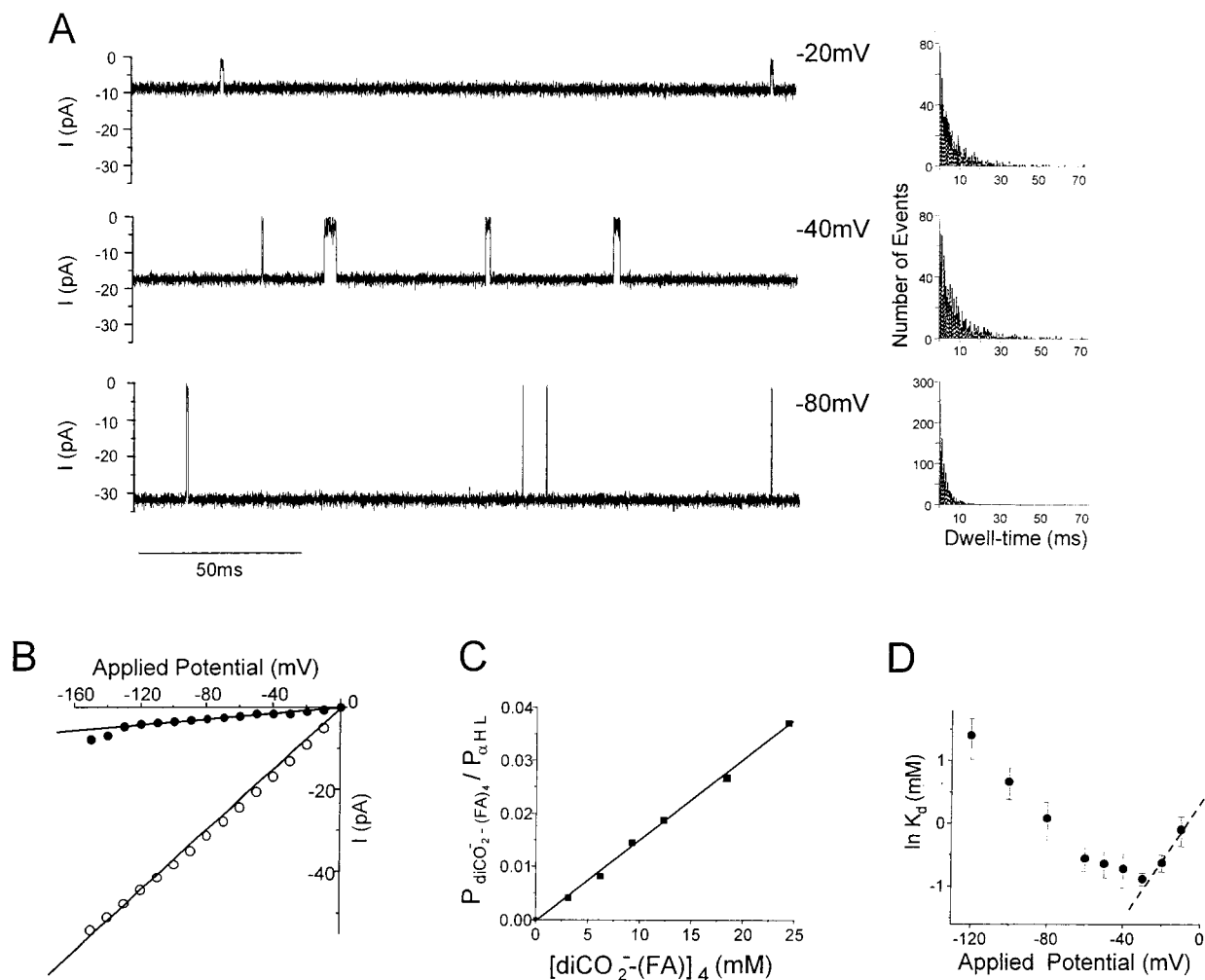


Figure 4. Interaction of the cyclic peptide $\text{diCO}_2^--(\text{FA})_4$ with the αHL pore. (a) Voltage dependence of binding of $\text{diCO}_2^--(\text{FA})_4$ to αHL . The $\text{diCO}_2^--(\text{FA})_4$ concentration was 3.1 mM. Dwell time histograms determined at: -20 , -40 , and -80 mV. Bessel filter, 5 kHz; acquisition rate, 100 kHz. (b) Residual current when $\text{diCO}_2^--(\text{FA})_4$ is lodged in the channel is proportional to the applied potential. I - V relationships for unoccupied αHL (○), and for αHL with $\text{diCO}_2^--(\text{FA})_4$ lodged in the channel lumen (●), measured in the same experiment. (c) The binding of $\text{diCO}_2^--(\text{FA})_4$ to αHL is concentration dependent. Plot of $P_{\text{diCO}_2^--(\text{FA})_4-\alpha\text{HL}}/P_{\alpha\text{HL}}$ versus the concentration of $\text{diCO}_2^--(\text{FA})_4$ in the *trans* chamber at an applied potential of -20 mV. (d) Voltage dependence of K_d for $\text{diCO}_2^--(\text{FA})_4$. The data at low applied potentials are fitted to eq 1 (dashed line).

Table 2. Kinetic Data for the Interaction of $\text{DiNH}_3^+(\text{FA})_4$ with the αHL Pore^a

V (mV)	k_{on} ($\text{M}^{-1} \text{s}^{-1}$)	k_{off} (s^{-1})	K_d (μM)
20	$0.87 (\pm 0.06) \times 10^6$	360 ± 10	420 ± 30
40	$0.92 (\pm 0.07) \times 10^6$	220 ± 20	240 ± 30
60	$0.98 (\pm 0.03) \times 10^6$	130 ± 10	140 ± 10
80	$1.1 (\pm 0.2) \times 10^6$	86 ± 7	81 ± 13
100	$1.3 (\pm 0.1) \times 10^6$	74 ± 18	56 ± 11
120	$1.2 (\pm 0.1) \times 10^6$	51 ± 2	43 ± 3

^aData are averaged from four experiments and given to two significant figures.

to the *cis* chamber at $+100$ mV. This led to the appearance of blocking events amounting to $97 \pm 2\%$ ($n = 4$) of the overall current, compared with the $62 \pm 1\%$ reduction seen with $\text{diNH}_3^+(\text{FA})_4$ alone. The frequency of the blocking events was linearly dependent upon the concentration of IP_6 (Figure 7), allowing the calculation of kinetic parameters for the binding of the IP_6 to $\alpha\text{HL} \cdot \text{diNH}_3^+(\text{FA})_4$ as a bimolecular process: $k_{\text{on}} = 3.4 (\pm 0.2) \times 10^6 \text{ M}^{-1} \text{ s}^{-1}$, $k_{\text{off}} = 1500 \pm 200 \text{ s}^{-1}$, $K_d = 450 \pm 10 \mu\text{M}$.

Discussion

In previous work, we showed that the properties of the pore formed by α -hemolysin (αHL) can be profoundly altered by

Table 3. Kinetic Data for the Interaction of $\text{DiCO}_2^--(\text{FA})_4$ with the αHL Pore^a

V (mV)	k_{on} ($\text{M}^{-1} \text{s}^{-1}$)	k_{off} (s^{-1})	K_d (μM)
-10	$1.6 (\pm 0.3) \times 10^5$	140 ± 20	900 ± 210
-20	$1.6 (\pm 0.1) \times 10^5$	83 ± 12	530 ± 70
-30	$2.0 (\pm 0.2) \times 10^5$	80 ± 7	410 ± 40
-40	$2.1 (\pm 0.6) \times 10^5$	94 ± 8	480 ± 130
-50	$2.2 (\pm 0.1) \times 10^5$	110 ± 20	520 ± 110
-60	$2.5 (\pm 0.6) \times 10^5$	140 ± 20	570 ± 100
-80	$3.0 (\pm 0.8) \times 10^5$	300 ± 30	1100 ± 300
-100	$3.3 (\pm 0.6) \times 10^5$	620 ± 110	1900 ± 500
-120	$3.4 (\pm 0.8) \times 10^5$	1300 ± 300	4000 ± 1300

^aData are averaged from four experiments and given to two significant figures

using cyclodextrins as noncovalent molecular adapters. Cyclodextrins lodge within the transmembrane β barrel of αHL where they alter conductance^{7,26} and ion selectivity,²⁶ and provide sites where channel blockers can bind.^{7,8}

To extend the range of molecules that might be used as adapters, we are examining classes of molecules other than cyclodextrins. Desirable attributes for adapters include dimensions similar to the inner diameter of the β barrel of αHL , the ability to act as hosts for guest molecules, and ease of synthesis as libraries of molecules with high purity. The cyclic peptides

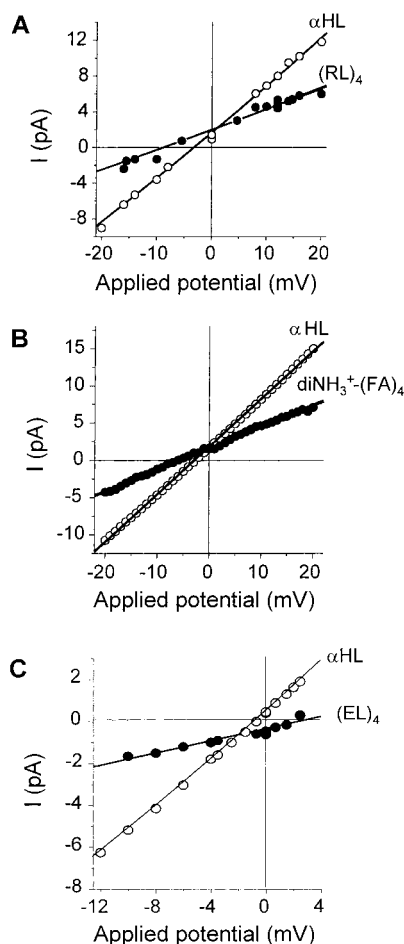


Figure 5. Charge selectivity of the α HL pore with $(\text{RL})_4$, diNH_3^+ -(FA) $_4$ or $(\text{EL})_4$ adapter peptides bound within the channel lumen. Reversal potentials were determined from the current–voltage (I – V) curves recorded under asymmetrical salt conditions: (○) unoccupied α HL; (●) α HL with bound adapter peptide. Representative experiments are shown. (a) α HL with $(\text{RL})_4$: *cis*, 1.3 M KCl; *trans*, 0.5 M KCl. (b) α HL with diNH_3^+ -(FA) $_4$: *cis*, 1.0 M KCl; *trans*, 0.5 M KCl. (c) α HL with $(\text{EL})_4$: *cis*, 0.9 M KCl; *trans*, 0.5 M KCl.

used here fulfill these requisites. They are based on the peptides originally used in the Ghadiri group to make nanotubes,⁴⁴ which can themselves act as transmembrane channels.^{27,28} The four cyclic peptides examined here do not form channels by themselves; rather they are charged and designed to cap nanotubes.³⁵ All four peptides contain eight alternating D- and L- α -amino acids. Molecular modeling and energy minimization with Insight II 98.0, assuming a dielectric constant of 78 and starting with peptide backbone structures determined by X-ray diffraction,³⁸ predict that flat disc conformations predominate for $(\text{RL})_4$ and $(\text{EL})_4$ in solution with outer diameters of 26.2 and 19.6 Å, respectively, and an inner diameter of 7.5 Å. β -Cyclodextrin by comparison has an outer diameter of 15.4 Å and an inner diameter of 6.2 Å. By contrast, the *N*-alkylated peptides, $(\text{diNH}_3^+$ -(FA) $_4$) and diCO_2^- -(FA) $_4$, which have less intramolecular charge repulsion and are more likely to form *cis* peptide bonds, may tend toward a more collapsed structure in solution. Finally, by comparison with the difficulties that can be encountered in the synthesis of many substituted cyclodextrins, cyclic peptides are more readily obtained in highly purified

form, and, importantly, libraries of cyclic peptides can be prepared.^{45–48}

Here we show that the four cyclic peptides bind in the lumen of the α HL pore and produce substantial reductions in the unitary conductance. The affinities of the peptides for α HL depend both on the charge of the peptide and the applied potential, suggesting that the peptides bind within the channel.^{40,41} As expected the positively charged peptides, $(\text{RL})_4$ and diNH_3^+ -(FA) $_4$, bind more tightly in a positive potential (with respect to the side of application of the peptide), while the negatively charged peptides, $(\text{EL})_4$ and diCO_2^- -(FA) $_4$, bind more tightly in a negative potential. The electrical distances (δ) for the site of peptide binding measured from the *trans* side of the bilayer were in the range 0.38–0.49 for the three peptides for which δ could be measured. Interestingly, at modest negative potentials (below –40 mV), the affinity of diCO_2^- -(FA) $_4$ for α HL is reduced, suggesting that the peptide is easily pushed through the channel under these conditions.^{49,50} The positively charged peptides behaved similarly, if less dramatically, at high positive potentials (above +120 mV). The extent to which the current is reduced by the peptides is 50–90%. The conductance of a transmembrane nanotube formed by eight-membered cyclic peptides is 65 pS under similar conditions,²⁸ as compared with the value of 500 pS for α HL. However, it is not possible to judge whether ion flow occurs through the center of the bound peptide rings under the present conditions, because the rather flexible peptides could assume closed conformations within the lumen of the α HL pore.

While lodged in the channel lumen, the cyclic peptides also change two additional properties of α HL, which are general characteristics of channel proteins. First, they alter the charge selectivity of α HL in keeping with simplistic predictions based on Coulombic interactions. α HL itself is weakly anion selective.^{10,26} The two positively charged peptides, $(\text{RL})_4$ and diNH_3^+ -(FA) $_4$, increase the anion selectivity, while the negatively charged peptide, $(\text{EL})_4$, converts α HL into a weakly cation-selective pore. Cation selectivity can also be produced by using the negatively charged hepta-6-sulfato- β -cyclodextrin as an adapter.²⁶ In addition, the bound peptides act as binding sites for channel blockers. Here, we focused on the two positively charged peptides, which can be induced to reside in the channel lumen for a few to tens of milliseconds at positive potentials, producing a stable reduction in channel current, and thereby permitting the observation of additional short blockades. Both $(\text{RL})_4$ and diNH_3^+ -(FA) $_4$ bound small negatively charged molecules including melittic acid, IP₆ and IP₃ with K_d values ranging from 131 μ M to 3.1 mM. These results reinforce the idea⁷ that noncovalent adapters are a versatile means by which to program the properties of α HL, and perhaps other channels and pores.

The nature of the interaction of the cyclic peptides with α HL cannot be rigorously defined at this stage in our investigations; we cannot yet say whether the peptides are held at a single binding site within the protein and, if they are, whether they are in a single conformation. Nevertheless, there are several

(45) Eichler, J.; Lucka, A. W.; Pinilla, C.; Houghton, R. A. *Mol. Diversity* **1996**, *1*, 233–240.

(46) Romanovskis, P.; Spatola, A. F. *J. Pept. Res.* **1998**, *52*, 356–374.

(47) Scott, C. P.; Abel-Santos, E.; Wall, M.; Wahnou, D. C.; Benkovic, S. J. *Proc. Natl. Acad. Sci. U.S.A.* **1999**, *96*, 13638–13643.

(48) Zhang, L.; Tam, J. P. *J. Am. Chem. Soc.* **1999**, *121*, 3311–3320.

(49) Choe, H.; Sackin, H.; Palmer, L. G. *J. Gen. Physiol.* **1998**, *112*, 433–446.

(50) Moczydlowski, E. Single-channel enzymology. In *Ion Channel Reconstitution*; Miller, C., Ed.; Plenum Press: New York, 1986; pp 75–113.

(44) Ghadiri, M. R.; Granja, J. R.; Milligan, R. A.; McRee, D. E.; Khazanovich, N. *Nature* **1993**, *366*, 324–327.

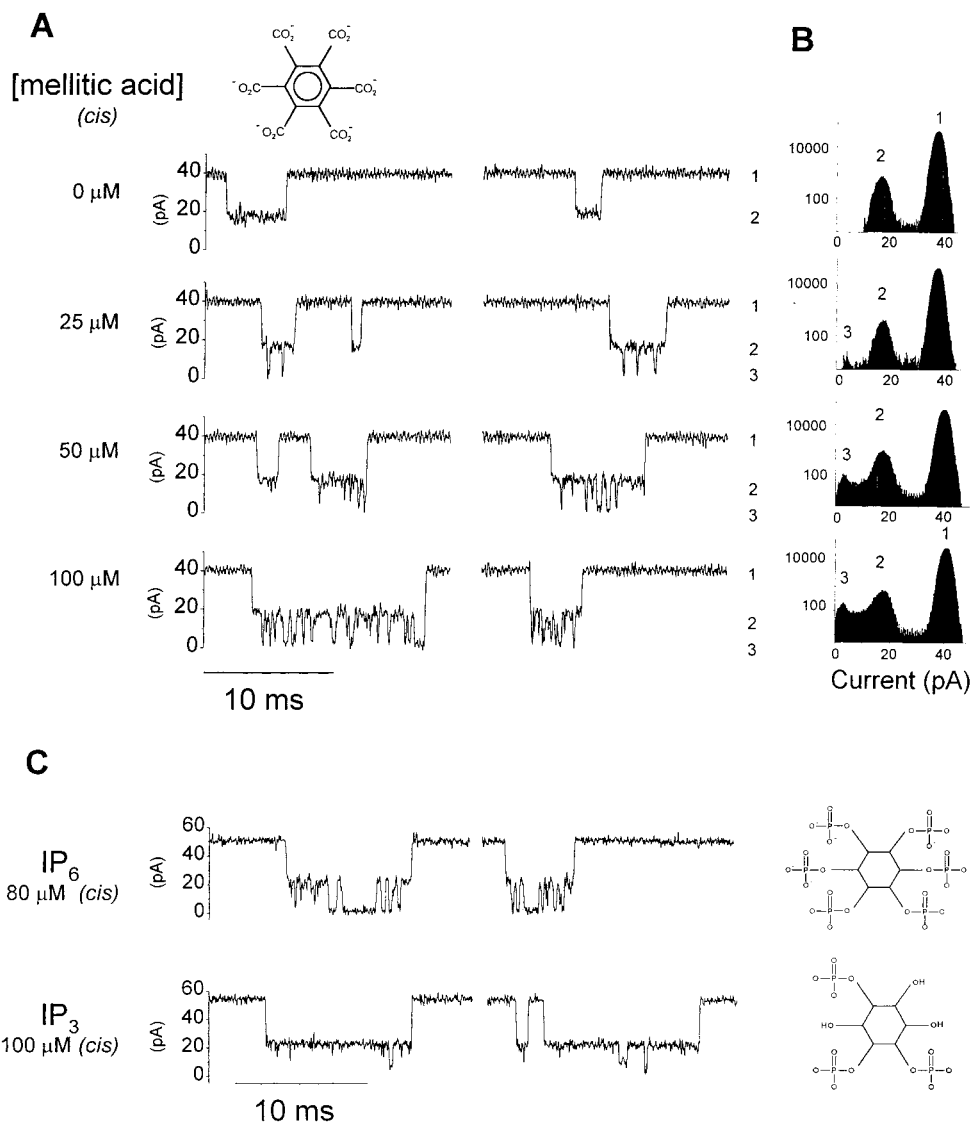


Figure 6. Effect of channel blockers on the current passed by αHL pores containing the $(\text{RL})_4$ adapter. (a) Dose–response of mellitic acid (*cis* chamber) in the presence of $6 \mu\text{M}$ $(\text{RL})_4$ in the *trans* chamber. Applied potential $+80 \text{ mV}$. Level 1, current through unoccupied αHL pore; level 2, current with $(\text{RL})_4$ lodged in the lumen; level 3, additional events attributed to the interaction of mellitic acid with $(\text{RL})_4$ within the channel lumen. (b) All-points semilogarithmic amplitude histograms from extended single-channel current traces in the presence of $6 \mu\text{M}$ $(\text{RL})_4$ and 0, 25, 50, and $100 \mu\text{M}$ mellitic acid. The designations of the peaks correspond to the levels shown in (a). (c) Comparison of the blockers phytic acid (IP_6) and *L*-myo-inositol 1,4,5-tris-phosphate (L-IP_3). Blockers were added to the *cis* chamber. $(\text{RL})_4$ was added to the *trans* chamber at $6 \mu\text{M}$ for the IP_6 experiment and at $8 \mu\text{M}$ for the IP_3 experiment. Bessel filter, 5 to 7 kHz; acquisition rate, 200 to 333 kHz.

arguments in favor of a single major site. First, the kinetics of the interactions of the peptides with αHL are in keeping with a simple bimolecular scheme. One exception is $\text{diNH}_3^+(\text{FA})_4$ at high concentrations, when two peptides appear to bind per αHL pore. Second, the dwell times of the peptides on the protein are quite long, certainly much longer than would be expected for the passage of a noninteracting or weakly interacting molecule through the pore.^{12,51–53} Third, the reduction of the unitary conductance is the same during each peptide interaction and does not vary during an encounter, implying the existence of a static conformation or, alternatively, rapid averaging on the microsecond time scale. The current does vary somewhat when $(\text{EL})_4$ is bound, suggesting a degree of mobility while it is lodged in the channel. Finally, the voltage-dependence of binding shows that the peptides $(\text{RL})_4$, $\text{diNH}_3^+(\text{FA})_4$, and

$\text{diCO}_2^-(\text{FA})_4$ are located at an electrical distance $\delta \approx 0.4–0.5$ from the *trans* entrance, that is, within the considerable limitations of this approach,⁴² close to the midpoint of the lumen, near the site of greatest constriction (Figure 1a). At this point, it is also unclear whether the polyanionic blockers bind in a specific orientation with respect to the peptides. Again, the simple bimolecular kinetics and uniform extents of block suggest that they do. Alternatively, polyanions moving from the *cis* to the *trans* side of the bilayer in the transmembrane potential may simply be involved in prolonged collisions with peptides retarded near the constriction at the center of the channel lumen.

The interactions between the αHL pore and the cyclic peptides that we have described here are especially promising, given that the peptides were originally designed for a different purpose.³⁵ We feel that improved peptides might be produced that would have a longer dwell time in the channel lumen. Since the crystal structure of the αHL pore is available,⁹ it may be possible, by molecular modeling, to engineer αHL pores that

(51) Bezrukov, S. M.; Vodyanoy, I. *Biophys. J.* **1993**, *64*, 16–25.

(52) Bezrukov, S. M.; Vodyanoy, I.; Parsegian, V. A. *Nature* **1994**, *370*, 279–281.

(53) Bezrukov, S. M. *J. Membr. Biol.* **2000**, *174*, 1–13.

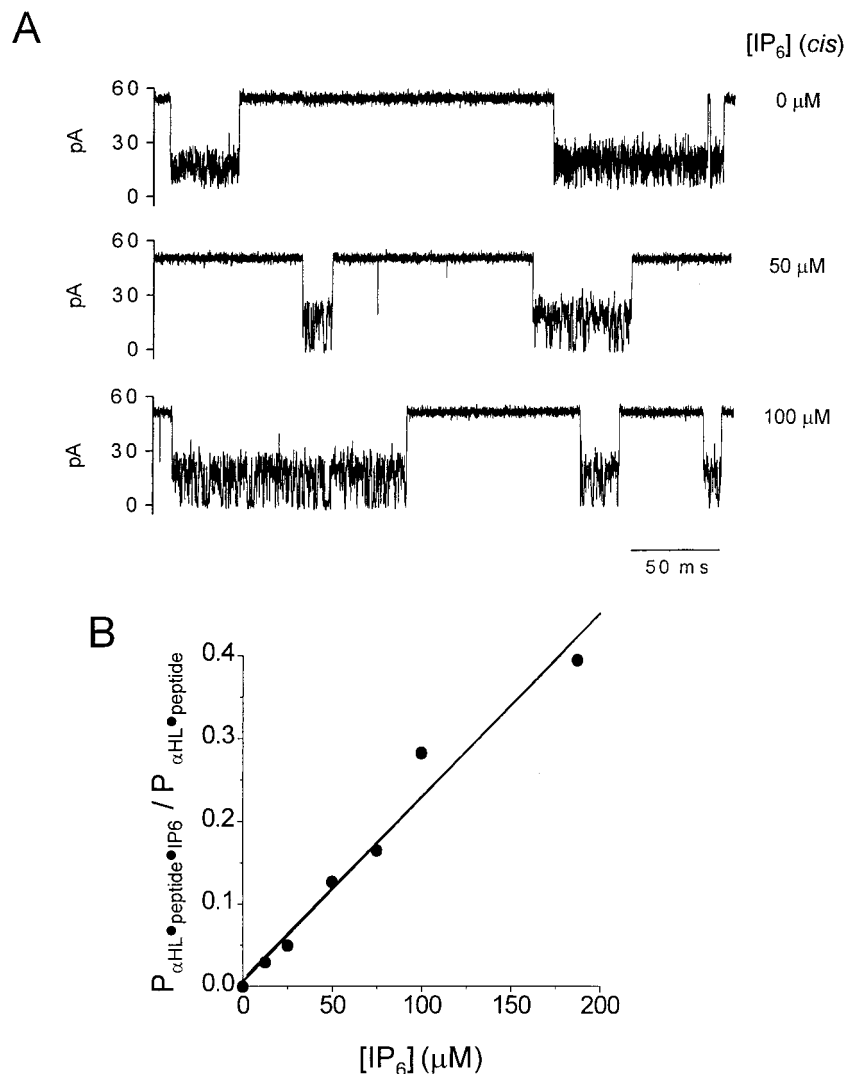


Figure 7. Effect of the blocker IP₆ on the current passed by αHL pores containing the diNH₃⁺-(FA)₄ adapter. (a) Typical traces obtained at +100 mV with a concentration of 6.1 μM of diNH₃⁺-(FA)₄ in the *trans* chamber and different concentrations of IP₆ in the *cis* chamber: 0, 50, and 100 μM. Bessel filter, 5 kHz; acquisition rate, 100 kHz. (b) Plot of $P_{\alpha\text{HL-peptide}\cdot\text{IP}_6}/P_{\alpha\text{HL-peptide}}$ versus the concentration of IP₆ in the *cis* chamber at an applied potential of +100 mV. The peptide concentration was 6.1 μM *trans*. Probabilities were calculated from the areas of all-points histograms.

better accommodate the peptides as we have done for β-cyclodextrin.⁷ It is also expected that more rigid, preorganized peptides will both bind to the pore lumen more tightly and interact with blockers more strongly.

αHL pores equipped with cyclic peptides that can bind analytes might have applications in stochastic sensing, where single-channel measurements are used both to identify and quantify molecules of interest.⁸ We have already shown that IP₃ can be detected, suggesting that the peptides might have a specific application in the detection of second messengers by

patch cramming, which uses intracellular electrodes containing responsive pores.⁵⁴

Acknowledgment. This work was supported by a MURI (ONR) award to H.B. and M.R.G. and by the ONR (H.B.). We thank Li-Qun Gu for helpful comments.

JA002436K

(54) Kramer, R. H. *Neuron* **1990**, *4*, 335–341.